05,13

Non-reciprocal propagation of spin waves in an asymmetric magnonic structure

© A.A. Grachev, A.V. Sadovnikov

Saratov National Research State University,
Saratov, Russia

E-mail: stig133@gmail.com

Received July 28, 2023
Revised September 13, 2023
Accepted September 26, 2023

This paper presents a study of spin-wave coupling effects in a parallel oriented magnetic microwaveguides made on yttrium iron garnet (YIG) films. The structure consists of two YIG microwaveguides separated by an air gap in the vertical direction, providing a dipole interaction between them, which has a shift relative to each other in the horizontal direction, forming an asymmetric geometry of vertically coupled microwaveguides. Micromagnetic calculation is used to demonstrate the phenomenon of non-reciprocal propagation of spin waves in the asymmetric geometry of vertically coupled microwaveguides. Based on the finite element method, the eigenmode spectrum of the considered structure is calculated under changing polarity of the external magnetic field, which demonstrates the change in dipole coupling of vertically coupled YIG microwaveguides. These results indicate that the manifestation of the non-reciprocal propagation of the spin waves is due to several factors. First, the asymmetric distribution of the internal magnetic field relative to the centers of each magnetic microwave. Second, the dependence of the overlap integral of the eigenmodes on the variation of the polarity of the external magnetic field. Micromagnetic modelling is used to show the transformation of the coupling length of the spin waves as the vertical spacing between the microwaves is varied. The results obtained in this work extend the possibilities of using the considered structure as a directional coupler for spin waves.

Keywords: nonreciprocity, magnonics, dipole interaction, coupled structures.

DOI: 10.61011/PSS.2023.11.57317.167

1. Introduction

The use of elementary quanta of magnetic excitations (magnons or spin waves (SW)) as carriers of information signals has recently attracted increasing interest due to the possibility of transferring the magnetic moment (spin) of an electron without transferring an electric charge and, therefore, without the heat release, which is inherent in semiconductor technologies [1,2]. Properties of SWs are determined by dipole and exchange interactions in magnetic media and can change significantly during the structuring of magnetic films. SWs are used in problems related to the generation [3], transmission [4], and processing [5,6] of macroscale and nanoscale information signals.

The creation of elementary blocks that perform a given set of signal processing functions (multiplexing and demultiplexing [7–9], signal division [10,11], spatial-frequency selection [12], linear [13] and nonlinear switching [14]) leads to the need to develop interconnection elements for efficient transmission of spin waves inside magnon networks [15,16], which are a topology of connected magnetic microscale and nanoscale structures.

The propagation of nonreciprocal SWs in magnon structures has acquired significant relevance in recent years due to their unique properties and potential applications of such structures [17–21]. The non-reciprocity is understood as an asymmetric transport of SWs, when their propagation is allowed in one direction and in the opposite direction it is blocked or suppressed. This feature opens up new opportunities for the development of promising magnonic devices with improved functional characteristics [18,19]. Non-reciprocal propagation [21–25] of SWs can be observed in magnetic waveguides with a tangential magnetization configuration (when the direction of the wave vector and the external magnetic field are perpendicular to each other in the plane of the film). In this case, the eigenmodes of the SWs propagating in the forward and backward directions can differ significantly due to the difference in the surface anisotropies of the magnetic field on the two film surfaces [23–25]. For multilayer waveguides, a classic object demonstrating nonreciprocity is a structure of two similar layers with antiparallel magnetization orientation [23,24]. Until now, the effect of non-reciprocal propagation of SWs has been considered only for magnetic waveguides with metallization [22] or for multilayer waveguides with different values of saturation magnetization [25]. In this case, these changes in magnetic media form the nonreciprocity of wave propagation regions.

This study proposes an asymmetric magnon structure based on two YIG microwaveguides separated by a vertical air gap that provides dipole interaction between them, and centers of the microwaveguides are shifted relative to each

other in the horizontal direction. Based on the conducted studies, it is shown that in an asymmetric magnon structure, the coupling length of spin waves is transformed when the gap between them changes, which results in the possibility of increasing the density of functional elements when designing multi-level magnon networks. Based on the finite element method, the spectrum of eigenmodes of the structure under consideration is calculated when the polarity of the external magnetic field changes, demonstrating a change in the dipole coupling of vertically coupled YIG microwaveguides.

2. Structure and micromagnetic modeling

Figure 1, *a* schematically shows the structure under consideration, which is a system of parallel oriented magnetic microwaveguides made from a film of yttrium iron garnet (YIG, $Y_3Fe_5O_{12}(111)$), with a thickness of $10\,\mu$m and a saturation magnetization of $4\pi M_0 = 1750$ G, the system is located on a gadolinium gallium garnet substrate (GGG, $Gd_3Ga_5O_{12}(111)$), with a thickness of $500\,\mu$m. YIG microwaveguides are identified as S_1, and S_2 and have widths of $w = 200\,\mu$m. The distance between the microwave guides is $s = 10\,\mu$m (see inset in Figure 1, *a*). The center of the microwave guide S_2 is shifted relative to the center of the microwave guide S_1 by the amount of $\xi = w/2$. The length (along the x axis) of the microwaveguide S_1 is 6 mm, and 5 mm is the length of the microwaveguide S_2. The structure is placed in a homogeneous static magnetic field with a magnitude of $H_0 = 1200$ Oe directed along the y axis. This configuration makes it possible to effectively excite magnetostatic surface waves (MSSW). Excitation of an MSSW propagating along the positive direction of x axis occurs in the microwave guide S_1, where the excitation region P_{in} is located.

It should be noted that when studying the propagation of SWs in transversely limited structures, it is important to take into account demagnetizing internal magnetic fields. Numerical modeling was performed in the MuMax3 software package and based on solving the Landau–Lifshitz–Gilbert (LLG) equation using the Dormand–Prince method [26]:

$$\frac{\partial \mathbf{M}}{\partial t} = \gamma\left[\mathbf{H}_{\text{eff}} \times \mathbf{M}\right] + \frac{\alpha}{M_0}\left[\mathbf{M} \times \frac{\partial \mathbf{M}}{\partial t}\right], \qquad (1.1)$$

where $\mathbf{M}$ is magnetization vector, $\alpha = 10^{-5}$ is attenuation parameter, $\mathbf{H}_{\text{eff}} = \mathbf{H}_0 + \mathbf{H}_{\text{demag}} + \mathbf{H}_{\text{ex}} + \mathbf{H}_{\text{a}}$ is effective magnetic field, $\mathbf{H}_0$ is external magnetic field, $\mathbf{H}_{\text{demag}}$ is demagnetization field, $\mathbf{H}_{\text{ex}}$ is exchange field, $\mathbf{H}_{\text{a}}$ is anisotropy field, $\gamma = 2.8$ MHz/Oe is gyromagnetic ratio in the YIG film. To reduce the signal reflection from the boundaries of the calculation area ($y = 0$ and $y = 8$ mm), regions were introduced in the calculation ($0 < y < 0.5$ mm and $5.5 < y < 6$ mm) with a coefficient α increasing geometrically. Due to the fact that the structure is placed in a magnetic field directed tangentially to the plane of each of the microwaveguides, the configuration of the static (equilibrium) magnetization and the wave excitation conditions determine the type of magnetostatic wave in the YIG film. Consequently, this magnetization geometry ensures the excitation of MSSW and the static magnetization will be oriented along the external magnetic field. The exchange constant in the YIG film is $A_{\text{ex}} = 3.612$ pJ/m. Moreover, within the framework of this problem, only the Zeeman energy of interaction of magnetic moments with an external field and dipole-dipole interaction inside the ferromagnet region are considered, which, together with the geometric limitations of the problem, determines the effect of shape anisotropy, which determines the inhomogeneous distribution of internal magnetic fields. The size of one grid cell was $5 \times 3 \times 2\,\mu\text{m}^3$ to eliminate the effect of inhomogeneous exchange. In this case, the calculation with a reduced cell size does not give significant changes in the resulted static and dynamic characteristics, which is explained by the fact that the wavelengths under consideration exceed by an order of magnitude the exchange length for YIG.

To excite propagating spin waves, a sinusoidal magnetic field of $h = h_0 \sin(2\pi f t)$ was applied to a section with a length of $100\,\mu$m with different oscillation amplitude h_0 and frequency f. $M_z(x, y, t)$ of each cell was recorded for 300 ns, which is sufficient to achieve a steady state. $m_z(x, y, t)$ oscillations were calculated for all cells by the following formula: $m_z(x, y, t) = M_z(x, y, t) - M_z(x, y, 0)$, where $M_z(x, y, 0)$ corresponds to the ground state.

Figure 1, *b, d, f, h* shows the results of micromagnetic modeling of the spin wave intensity distribution proportional to the squared value of the dynamic magnetization $I(x, y) = \sqrt{m_x^2 + m_z^2}$, Figure 1, *e, g, i* shows distributions of the dynamic magnetization component m_z at a frequency of $f = 5.30$ GHz. Figure 1, *b*–*e* shows the case for a vertical gap of $s = 10\,\mu$m, the maps in Figure 1, *b, c* were taken for the layer that corresponds to the microwaveguide S_1, and maps in Figure 1, *d, e* were taken for the layer that corresponds to the microwaveguide S_2. From the data obtained, it can be seen that the power of the spin wave is pumped from the microwaveguide S_1 to the microwaveguide S_2 over a distance along the x axis equal to the coupling length L, which coincides numerically with the distance where the SW energy is transferred from the strip S_1 to the strips S_2. It is important to note that in both microwaveguides the SW beam propagates asymmetrically relative to the center of each microwaveguide. An increase in the vertical gap up to $s = 60\,\mu$m (see Figure 1(*f*–*i*)) results in almost 2 times increase in the coupling length L and also the asymmetry of the SW beam propagation in microwaveguides almost disappears in the system.

Then the internal magnetic fields were calculated along the width of microwaveguides. Figure 1, *j, k* shows the profiles of the internal magnetic field of YIG microwaveguides in the section $x = 3$ mm upon changes in the gap value s. It

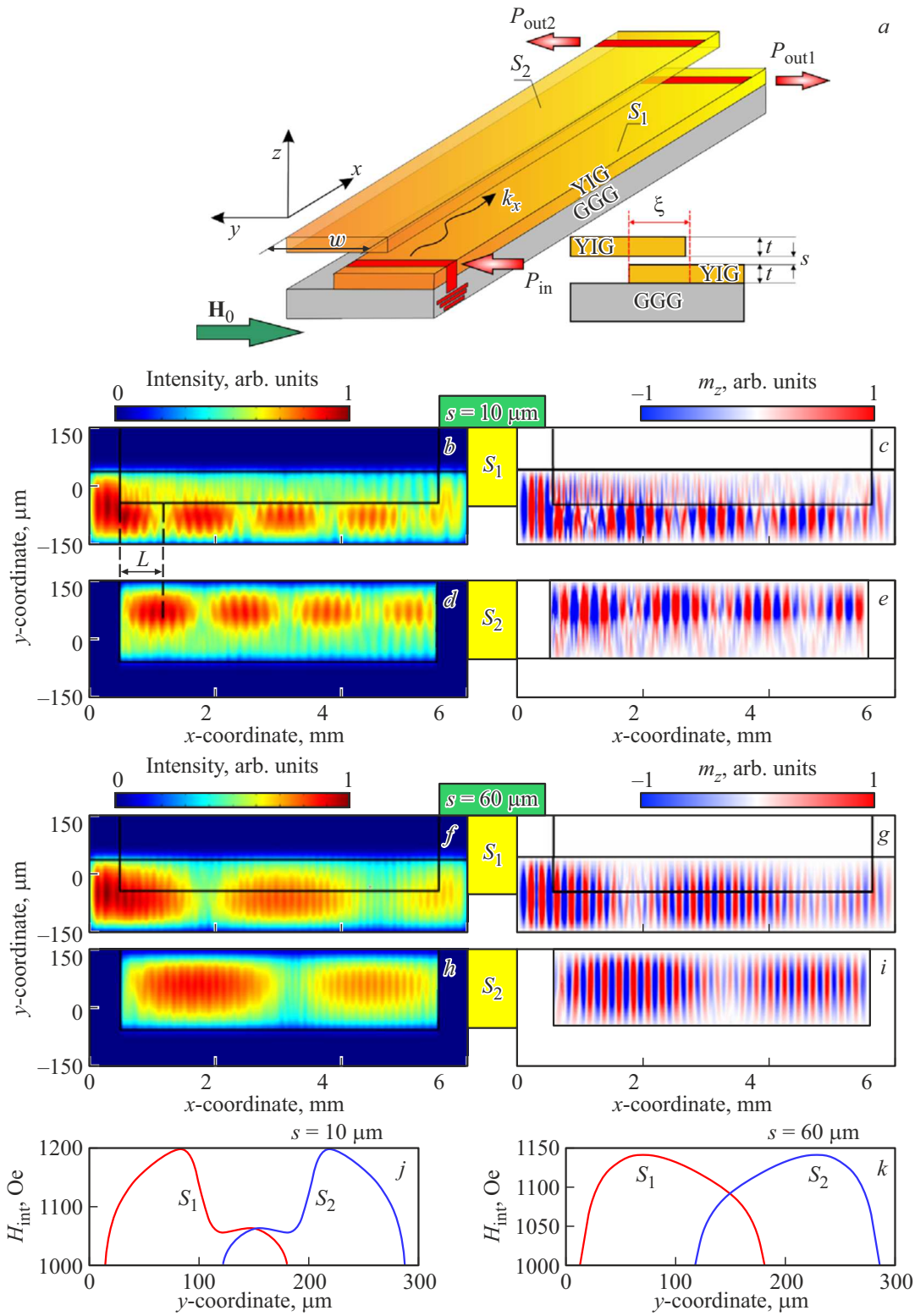

Figure 1. (*a*) Schematic diagram of an asymmetric magnon structure. (*b*–*i*) Left panels show the spin wave intensity distributions proportional to the square of the dynamic magnetization, right panels show distributions of the dynamic magnetization component m_z. (*b*–*e*) The case of vertical gap $s = 10\,\mu$m. (*f*–*i*) The case of vertical gap $s = 60\,\mu$m. The data is given for $H_0 = 1200$ Oe and an input signal frequency of $f = 5.3$ GHz. Profiles of the internal magnetic field of microwaveguides for vertical gaps of $s = 10\,\mu$m (*j*) and $s = 60\,\mu$m (*k*).

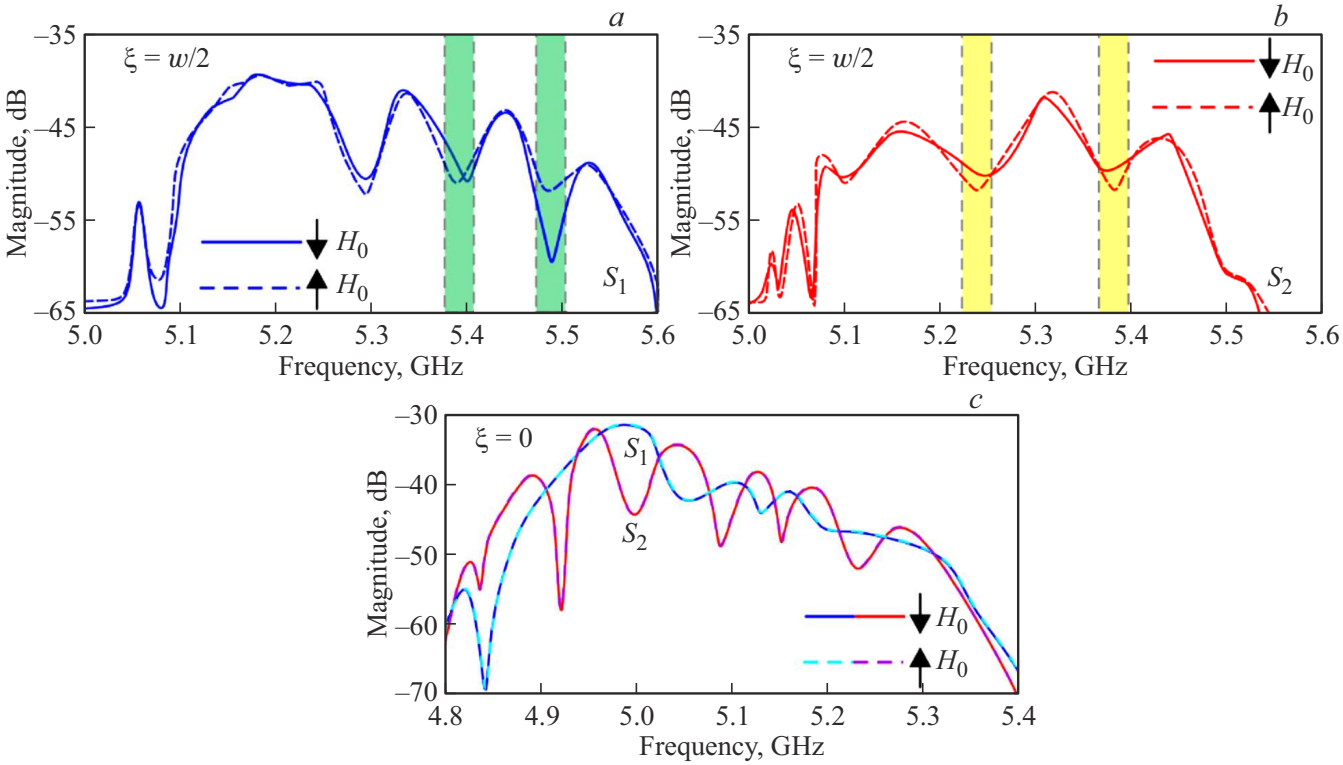

Figure 2. (a) Schematic diagram of an asymmetric magnon structure. (b–i) Left panels show the spin wave intensity distributions proportional to the square of the dynamic magnetization, right panels show distributions of the dynamic magnetization component m_z. (b–e) The case of vertical gap $s = 10\,\mu$m. (f–i) The case of vertical gap $s = 60\,\mu$m. The data is given for $H_0 = 1200$ Oe and an input signal frequency of $f = 5.3$ GHz. Profiles of the internal magnetic field of microwaveguides for vertical gaps of $s = 10\,\mu$m (j) and $s = 60\,\mu$m (k).

can be seen that with a gap of $s = 10\,\mu$m (see Figure 1,j) there is a strong transformation of profiles H_{int} in both microwaveguides in the form of a sharp decrease in the internal magnetic field in the area of intersection of YIG-microwaveguides. In this case, the asymmetry in the distribution of H_{int} does not prevent the SW pumping between the microwaveguides, thus, in the coupled system, two waveguide channels are formed in each of the YIG microwaveguides, which are asymmetrical relative to their centers. With a gap of $s = 60\,\mu$m, the distribution of H_{int} for each microwaveguide is nearly leveled off at the center of each of them. We will refer to this geometry as an asymmetric magnon structure. It should be added that the term „asymmetric“ here means an asymmetric arrangement of microwaveguides: relative to their centers and the creation of an asymmetric profile of the internal magnetic field distribution in them.

It should be noted that electromagnetic waves propagating in structures with gyrotropic media have the property of nonreciprocity, i.e. the dependence of wave number on the direction of propagation. And if another microwaveguide is added on top of the microwaveguide in question and the added one is shifted relative to the center of the later, this will cause an asymmetry in the distribution of the internal magnetic field and lead to the emergence of areas of non-reciprocal SW propagation in the system under consideration.

To demonstrate the non-reciprocal propagation of SW in an asymmetric magnon structure, the frequency dependences of the power spectral density were calculated when the polarity of the external magnetic field changed. For this purpose, the input signal was defined in the form of $h_z(t) = h_0 \sin c(2\pi f_c t)$ with a central frequency of $f_c = 7$ GHz, $h_0 = 0.1$ Oe. Then the value of dynamic magnetization $m_z(x, y, t)$ in the output regions $P_{\text{out1,2}}$ was recorded with a step of $\Delta t = 75$ fs for $T = 500$ ns. As a result, it was possible to plot the frequency dependence of the dynamic magnetization of the output regions $P_{\text{out1,2}}$ using the Fourier transform.

Figure 2,a, b shows frequency spectra of the SW signal at the output regions of microwaveguides S_1 (see Figure 2,a) and S_2 (see Figure 2,b) for cases of negative (solid curves) and positive (dashed curves) direction of the external magnetic field relative to y axis. These results are shown for the case of the shift of $\xi = w/2$. A change in the polarity of the external magnetic field results in a redistribution of the spin wave signal power in microwaveguides in the areas of frequency dips (see green and yellow areas in Figure 2,a, b),

corresponding to the transfer of spin wave power between YIG microwaveguides. It can be noted that for the microwaveguide S_1 a change in the polarity of the external magnetic field leads to an increase in the transmission of SW power (approximately 10 dB) in the range from 5.47 to 5.5 GHz. This fact demonstrates the frequency tuning of the SW propagation modes in the proposed magnon structure: by changing the polarity of the external magnetic field. At the same time, if the case of two vertically coupled microwave guides at $\xi = 0$ is considered (see Figure 2, *c*), then the main difference can be noticed: this system lacks non-reciprocal propagation of SWs.

It should also be noted that the phenomenon of non-reciprocal SW propagation can be associated with two factors. The first factor is the highly inhomogeneous asymmetric distribution of the internal magnetic field. The second factor is the presence of a distributed dipole coupling between magnetic microwaveguides in the vertical direction, which results in a change in the precession trajectory of the magnetic moment [20] and ellipticity [27] of the motion of spin moment precession along the width of the YIG-microwaveguides.

3. Calculation of the spectrum of eigenmodes

Due to the fact that the micromagnetic modeling method does not allow obtaining to the fullest possible extent the information about the spectrum of eigenmodes of the spin waves propagating in the structure under consideration, the electrodynamic properties of the asymmetric magnon structure were calculated using the finite element method [28,29], in the Comsol Multiphysics software package. When modeling in the frequency domain, all components of the electromagnetic field depend on frequency following the $e^{i\omega t}$ law. In this case, Maxwell's equations for the electric field strength vector $\mathbf{E}$ yield the following equation

$$\nabla \times (\hat{\mu}^{-1} \nabla \times \mathbf{E}) - k^2 \varepsilon \mathbf{E} = 0, \qquad (1.2)$$

where $k = \omega/c$ is wave number in vacuum, $\omega = 2\pi/f$ is circular frequency, f is frequency of the electromagnetic wave.

The following parameters were used in the calculation: dielectric constants of the GGG substrate and the YIG microwaveguides were assumed to be equal to $\varepsilon_{GGG} = 9$ and $\varepsilon_{YIG} = 14$, respectively, and the magnetic permeability tensor $\hat{\mu}(f)$ of YIG strips was taken as

$$\hat{\mu}(f) = \begin{vmatrix} \mu(f)\sin^2\varphi + \cos^2\varphi & i\mu_a(f)\sin\varphi & (1-\mu(f))\sin\varphi\cos\varphi \\ -i\mu_a(f)\sin\varphi & \mu(f) & i\mu_a(f)\cos\varphi \\ (1-\mu(f))\sin\varphi\cos\varphi & -i\mu_a(f)\cos\varphi & \mu(f)\cos^2\varphi + \sin^2\varphi \end{vmatrix},$$

where

$$\mu(f) = \frac{f_\perp^2 - f^2}{f_H^2 - f^2}, \quad \mu_a(f) = \frac{f_M f}{f_H^2 - f^2},$$

$$f_M = \gamma 4\pi M_0 = 4.9\,\text{GHz}, \quad f_H = \gamma H_0 = 3.36\,\text{GHz},$$

$$f_\perp = \sqrt{f_H(f_H + f_M)} = 5.26\,\text{GHz}$$

where is frequency of transverse ferromagnetic resonance in a tangentially magnetized ferrite film, $\varphi = \pm 90^\circ$ is angle of direction of the external magnetic field relative to x axis. The spectrum of eigenmodes of a vertically coupled structure consists of an orthogonal system of symmetric (see Figure 3, *a*) and antisymmetric modes (see Figure 3, *b*) with the corresponding wave numbers Φ_S, and Φ_{AS}. When the polarity of the external magnetic field changes, the mode distributions (see Figure 3, *c*, *d*) are localized in the region between the magnetic microwaveguides. There is also a relative change in the intensity of distributions when the polarity of the external magnetic field changes, because all four distributions are based on the same numerical interval H_z. These results may also be indicative of a change in the energy of spin waves and wave numbers of eigenmodes, and hence the spin-wave dispersion as a whole, which consists well with the results of micromagnetic modeling. Moreover, if the distribution of the magnetic field component H_x is plotted (see Figure 3, *e*), it can be seen that the distribution of the magnetic field (distribution of $\vec{\mathbf{H}}$ is shown with arrowed lines) inside magnetic microwaveguides is uneven in thickness and also transformed at the edges. This fact also causes non-reciprocal propagation of SW in the system.

Moreover, when proceeding to the case that occurs in a tangentially magnetized ferrite microwave guide when the orientation of the magnetic field changes to the opposite one and considering the transverse structure of the wave field (deducing the field distribution along the thickness of the microwave guide) [30], it results in a change in the area inside the microwaveguide where the maximum magnetic field component is observed. In this case, a vector can be introduced normal to the film surface $\mathbf{n} = \pm 1$, near which the maximum magnetic field component is observed. When the direction of the external magnetic field changes, the mode shifts from one surface of the microwaveguide to another. In the case of a shift vector ξ of one of the microwaveguides relative to the other, and co-directed with the magnetic field strength vector $\xi \parallel \mathbf{H}$, no symmetry changes will be observed in the symmetry properties of spin waves propagating along the system of microwaveguides (triples of vectors $\mathbf{k}$, $\mathbf{H}$, $\mathbf{n}$ and $\mathbf{k}$,

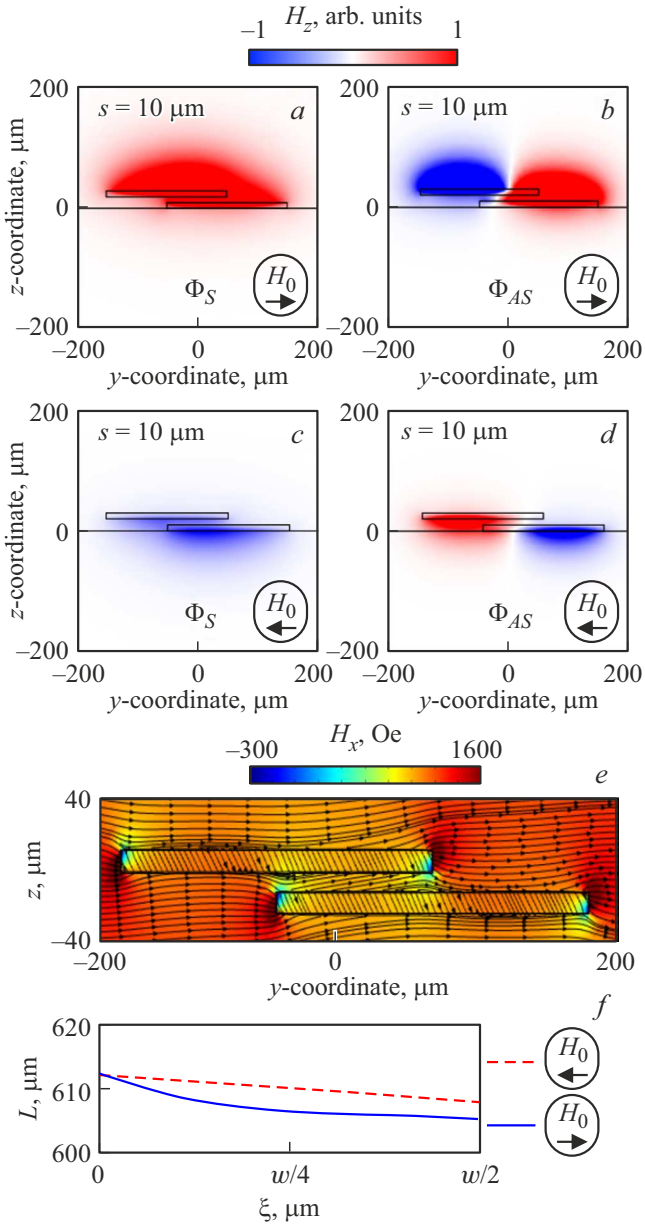

Figure 3. (a–d) Distributions of the magnetic field component H_z for eigenmodes of an asymmetric magnon structure. The data is given for $H_0 = 1200$ Oe and an input signal frequency of $f = 5.3$ GHz. Two-dimensional map of the spatial distribution of the H_x-component of the magnetic field in the asymmetric magnon structure. The distribution of $\hat{\mathbf{H}}$ is shown with arrowed lines. The dependence of L as a function of the shift between the centers of the microwave guides ξ for the cases of the external magnetic field directed toward the negative (dashed red curve) and positive (solid blue curve) side relative to the y axis.

ξ, **n** will be right-handed), however, the distribution of eigenmode field profiles will change when the orientation of the magnetic field changes to the opposite. This fact causes nonreciprocity in the regions of wave propagation in the waveguide structure formed by thin-film sheared ferrite microwaveguides.

Figure 3,f shows the dependence of the coupling length

$$L = \frac{\pi}{|\Phi_S - \Phi_{AS}|}$$

on changes in the shift value between the centers of the microwaveguides ξ. It is important to note that changing the value of ξ from 0 to $w/2$ results in a decrease in L by $5\,\mu$m. When the polarity of the external magnetic field changes, a slight change in the values of L is observed, especially in the region of $\xi = w/2$. This fact also confirms that in an asymmetric arrangement of magnetic strips, the overlap of the integral of the eigenmodes depends on the direction of the external magnetic field. Thus, it can be said that the proposed system has sufficient sensitivity in the conditions of changing parameters, such as shift ξ, relative to the centers of the microwaveguides. The use of the phenomenon of non-reciprocal SW propagation is a significant advantage over photonics devices [31,32].

4. Conclusion

Thus, using numerical studies, spin-wave transport in an asymmetric magnon structure in the form of vertically coupled YIG microwaveguides has been demonstrated. Based on micromagnetic modeling and the finite element method, the amplitude-frequency characteristics of the SW and the spectra of the eigenmodes of the asymmetric magnon structure were obtained. It is shown that changing the polarity of the external magnetic field leads to a change in the coupling between the YIG microwaveguides. These results indicate the manifestation of non-reciprocal propagation of spin waves from several factors. First, the asymmetric distribution of the internal magnetic field relative to the center of each magnetic microwaveguide, creating regions of non-reciprocal SW propagation. Second, the dependence of the overlap integral of eigenmodes on changes in the polarity of the external magnetic field. Using micromagnetic modeling, the transformation of the spin wave coupling length is shown when the vertical gap between the microwaveguides changes. The results obtained in this study expand the possibilities of using the structure considered as a directional spin wave coupler.

Funding

This study was supported by a grant of the Russian Science Foundation (project No. 23-79-30027).

Conflict of interest

The authors declare that they have no conflict of interest.

References

[1] A. Barman, G. Gubbiotti, S. Ladak, A.O. Adeyeye, M. Krawczyk, J. Grafe, C. Adelmann, S. Cotofana, A. Naeemi, V.I. Vasyuchka, B. Hillebands. J. Phys.: Condens. Matter **33**, 413001 (2021).

[2] S.A. Nikitov, A.R. Safin, D.V. Kalyabin, A.V. Sadovnikov, E.N. Beginin, M.V. Logunov, M.A. Morozova, S.A. Odintsov, S.A. Osokin, A.Yu. Sharaevskaya, Yu.P. Sharaevsky, A.I. Kirilyuk. Phys. Usp. **63**, 945 (2020).

[3] A.V. Kondrashov, A.B. Ustinov, B.A. Kalinikos, Pisma v ZhTF **36**, *5*, 62 (2010). (in Russian).

[4] S.J. Hämäläinen, M. Madami, H. Qin, G. Gubbiotti, S. van Dijken. Nature Commun. **9**, *1*, 4853 (2018).

[5] G. Csaba, Á. Papp, W. Porod. Phys. Lett. A **381**, *17*, 1471 (2017).

[6] M. Balinskiy, H. Chiang, A. Khitun. Aip Adv. **8**, 5 (2018).

[7] Yu.K. Fetisov, A.S. Sigov, Radioelektronika. Nanosistemy. Informatsionnyie tekhnolgii **10**, *3*, 343 (2018). (in Russian).

[8] K. Vogt, F.Y. Fradin, J.E. Pearson, T. Sebastian, S.D. Bader, B. Hillebrands, A. Hoffmann, H. Schultheiss. Nature Commun. **5**, 3727 (2014).

[9] Z. Zhang, M. Vogel, J. Holanda, M.B. Jungfleisch, C. Liu, Y. Li, J.E. Pearson, R. Divan, W. Zhang, A. Hoffmann, Y. Nie, V. Novosad. Appl. Phys. Lett. **115**, 232402 (2019).

[10] G.M. Dudko, A.V. Kozhevnikov, Yu.V. Khivintsev, Yu.A. Filimonov, A.G. Khitun, S.A. Nikitov, Radiotekhnika i elektronika **63**, *10*, 1105 (2018). (in Russian).

[11] X.S. Wang, Y. Su, X.R. Wang. Phys. Rev. B **95**, 014435 (2017).

[12] Y. Hashimoto, D. Bossini, T.H. Johansen, E. Saitoh, A. Kirilyuk, T. Rasing. Phys. Rev. B **97**, 140404(R) (2018).

[13] R. Gieniusz, P. Gruszecki, M. Krawczyk, U. Guzowska, A. Stognij, A. Maziewski. Sci. Rep. **7**, 8771 (2017).

[14] H.G. Bauer, P. Majchrak, T. Kachel, C.H. Back, G. Woltersdorf. Nature Commun. **6**, 8274 (2015).

[15] Y. Khivintsev, V. Sakharov, A. Kozhevnikov, G. Dudko, Y. Filimonov, A. Khitun. J. Magn. Magn. Mater. **545**, *11*, 168754 (2022).

[16] Three-dimensional magnonics: layered, micro-and nanostructures / Ed. G. Gubbiotti. CRC Press (2019).

[17] M. Jamali, J.H. Kwon, S.-M. Seo, K.-J. Lee, H. Yang. Sci. Rep. **3**, 1 (2013).

[18] J. Chen, H. Yu, G. Gubbiotti. J. Phys. D **55**, 123001 (2021).

[19] H. Wang, J. Chen, T. Yu, C. Liu, C. Guo, S. Liu, K. Shen, H. Jia, T. Liu, J. Zhang. Nano Res. **1** (2020)

[20] P. Deorani, J.H. Kwon, H. Yang. Current Appl. Phys. **14**, S129 (2014).

[21] F. Vanderveken, H. Ahmad, M. Heyns, B. Soŕee, C. Adelmann, F. Ciubotaru. J. Phys. D **53**, 495006 (2020).

[22] O. Gladii, M. Haidar, Y. Henry, M. Kostylev, M. Bailleul. Phys. Rev. B **93**, *5*, 054430 (2016).

[23] P.A. Grünberg. Rev. Mod. Phys. **80**, 1531 (2008).

[24] R.A. Gallardo, T. Schneider, A.K. Chaurasiya, A. Oelschlägel, S.S.P.K. Arekapudi, A. Roldán-Molina, R. Hübner, K. Lenz, A. Barman, J. Fassbender, J. Lindner, O. Hellwig, P. Landeros. Phys. Rev. Appl. **12**, 034012 (2019).

[25] S. Odintsov, S. Sheshukova, S. Nikitov, E. Lock, E. Beginin, A. Sadovnikov. J. Magn. Magn. Mater. **546**, 168736 (2022).

[26] A. Vansteenkiste, J. Leliaert, M. Dvornik, M. Helsen, F. Garcia-Sanchez, B. Van Waeyenberge. AIP Advances **4**, 107133 (2014).

[27] M. Krawczyk, D. Grundler. J. Phys.: Condens. Matter **26**, 123202 (2014).

[28] P.P. Silvester, R.L. Ferrari. Finite Elements for Electrical Engineers. Cambridge University Press (1996). 541 p.

[29] O.C. Zienkiewicz, R.L. Taylor, J.Z. Zhu. The finite element method: its basis and fundamental. Elsevier (2005).

[30] D.D. Stancil, A. Prabhakar. Spin waves, N.Y. Springer Sci. (2009).

[31] S. Yoo, B. Guan, R.P. Scott. Microsystems Nanoeng. **2**, 1 (2016).

[32] X. Mu, S. Wu, L. Cheng, H. Fu. Appl. Sci. **10**, 1538 (2020).

Translated by Y.Alekseev